Experimental and Modeling Study on Nighttime Heat Loss and Anti-Freezing Analysis of FPC Group

Zhenghao Jin[1], Yin Zhang[2], Yanru Li[2], Fei Liang[2], Xinhui Zhao[2], Qinjian Liu[2], Enshen Long[1,2,*]

[1]Institute for Disaster Management and Reconstruction, Sichuan University, Chengdu, Sichuan, 610065, China

[2]College of Architecture and Environment, Sichuan University, Chengdu, Sichuan, 610065, China

Abstract

The low-temperature-caused freezing of outdoor pipes and solar collectors in winter night is one of the most serious problems in solar thermal system. Studying the heat loss characteristic of the solar connector groups in nighttime is greatly significant for solar collector groups anti-freezing and maintaining system safety. In this paper, a heat loss mathematical model was established and validated through on-site measurement, to investigate the heat loss characteristic of the flat plate solar collectors (FPC) groups. Furthermore, the anti-freezing critical flow rate was analyzed when outdoor temperature and inlet water temperature vary. As an illustrative example, the anti-freezing analysis for Harbin, a northern city in China, was conducted. The results show that, the front heat loss and connecting pipes constituted the main heat loss of the solar collector group in nighttime, which accounted for 63.32% and 15.53% respectively. Besides, making anti-freezing flow rate equal to daytime working design flow rate is not suitable. Hence, the flow rate should be reduced through the water pump frequency conversion methods. Moreover, winter minimum temperature in China severe cold area can be 28.7℃. On that occasion, a single set of solar connector group should keep the inlet temperature higher than 15℃, while the flow rate larger than 0.5L/min.

Keywords: flat plate solar collectors, nighttime heat loss, heat loss mathematical model, anti-freezing

1. Introduction

With the extensive use of fossil fuels, global pollution problem is getting increasingly serious. The use of renewable energy has been paid more and more attention to by many countries around the world, in which the solar energy is promoted for the similarity to that of traditional energy maneuverability and adaptability (F. Dinter and Mayorga Gonzalez, 2014; Xiaolei Li et al., 2017) . Solar energy utilization can be either photovoltaic or photothermal. While the hot water system, which is a kind of photothermal, is of high working stability and easy for thermal energy storage, making it suitable for heating in winter (BillyAnak Sup et al., 2014; CJ Porras-Prieto et al., 2014; L.M. Ayompe et al., 2011). However, in severely cold areas, the freezing of outdoor pipes and collectors is one of the most serious problems, which, to a certain degree, limits the utilization of solar energy and decreases the system economic performance (Huifang Liu et al., 2015). As a result, studying the heat loss characteristic of the solar connector groups at night to avoid frost crack and maintain the system working safe and stable really makes a great difference.

According to available literatures, many scholars studied the solar connector anti-freezing. The conventional measures include the use of antifreeze fluid, electric tracing tapes, draining water from the collectors and using the hot water in a thermal storage tank to heat the outdoor pipes by circulation (BV Bourke, 1995; HMS Hussein et al., 1999; M Smyth et al, 2001; PW Cronin et al., 1997; R.H. Lewis and JB Carr, 1981). For FPC, KLEINS (S.A. Klein, 1975) proposed a method to calculate the heat loss coefficient, and respectively, put forward the top, bottom and side heat loss coefficient calculation method. Gao Liuhua (Gao Liuhua et al., 2014) proposed a one-dimensional steady state mathematic model of single FPC. He took overall heat loss coefficient of collector as a variable quantity. And absorber plate thickness and tube spacing of copper-aluminum FPC were optimized based on efficiency factor and metal consumption of collector. Th Beikircher (Th. Beikircher et al., 2014) studied heat loss measurements without insolation and a novel conversion towards daytime conditions. This research thought a broader application and test of the new method for further types of solar collectors by independent researchers is desirable. Fan Zhou (Fan Zhou et al., 2017) did experimental and numerical study of the freezing process of

doi:10.18086/swc.2017.31.06 Available at http://proceedings.ises.org

FPC, finding that narrowing the pipe space, increasing the pipe diameter or header diameter and reducing the emissivity of absorber and glass-cover are the effective ways of enhancing the antifreeze performance of flat-plate collector. But the reported studies rarely analyze the influence of the environment temperature, the inlet temperature, and the flow rate to a FPC group anti-freezing.

In this paper, a heat loss mathematical model was established and validated through on-site measurement, to study the heat loss characteristic of the FPC groups. Furthermore, the anti-freezing critical flow rate was analyzed when outdoor temperature and inlet water temperature vary. And we had an anti-freezing analyze of Harbin as a typical case. This study can provide meaningful references for practical engineering.

2. Experimental System

In order to study the heat loss characteristic of FPC groups in nighttime, we built a test bench at Sichuan University, which is at east longitude 30.67° and north latitude 104.06°. Fig.1 is the schematic diagram of the experiment system. From the figure, the test bench includes two FPC groups, which can control the flow rate independently. Besides, each FPC group is set up by two pieces of 2000mm×1000mm×700mm FPCs in parallel. The FPCs is facing south while the installation angle is 40°. Within each FPC group, the connecting pipes between two FPC is 74mm long and is made of copper.

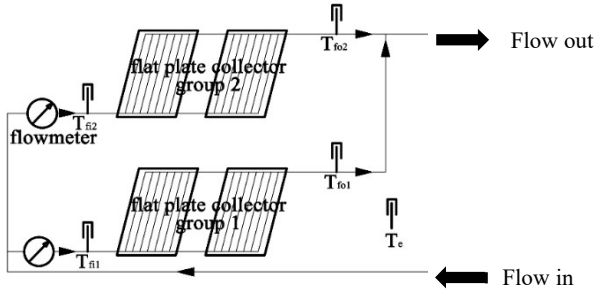

Fig.1 experiment system diagram

Fig.2 is the FPC configuration diagram, which shows the PFC comprises glass cover-plate, sheet absorber, pipe, insulating layer and housing. The sheet absorber is made of pure aluminum anodic oxide film plating. The insulating layer is made of polyurethane foam. And the pipe is made of copper. The heat loss of FPC can be divided into front heat loss, bottom heat loss, and side heat loss. Tab.1 shows detailed parameters for the FPC and connecting pipes.

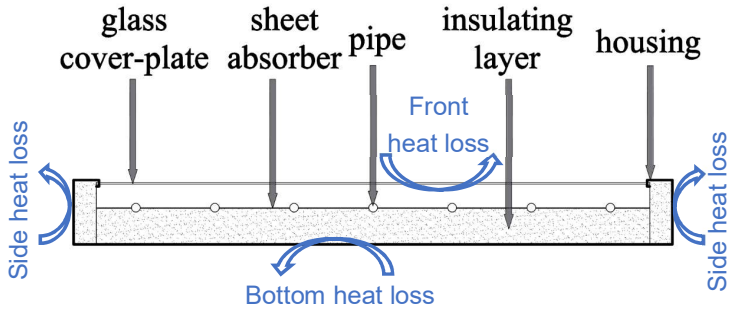

Fig.2: FPC configuration diagram

Tab. 1: Detailed parameters for the FPC and connecting pipe

Item	Value	Item	Value
FPC length /mm	2000	Connecting pipe number	2
FPC width/mm	1000	Connecting pipe length/m	0.074
FPC thickness/mm	70	Connecting pipe thermal	386.4

		conductivity/W·(m·K)$^{-1}$	
FPC lighting area /m2	1.85	FPC pipe outer diameter / mm	8
Sheet absorber length/mm	1940	FPC pipe wall thickness /mm	0.5
Sheet absorber width/mm	950	FPC pipe thermal conductivity / W·(m·K)$^{-1}$	386.4
Sheet absorber thickness/mm	0.4	Glass cover-plate emissivity	0.9
Sheet absorber emissivity	0.09	Glass cover-plate number	1
Sheet absorber absorptivity	0.95	Insulating layer thermal conductivity / W·(m·K)$^{-1}$	0.023
Sheet absorber thermal conductivity /W·(m·K)$^{-1}$	202.8	Bottom insulating layer thickness /mm	20
Connecting pipe outer diameter / mm	22	Side insulating layer thickness /mm	20
Connecting pipe wall thickness /mm	0.6		

The pipe between temperature measuring point and inlet or outlet water gates for FPC group is short and has a good thermal insulation, so it is assumed that the tested temperature is the temperature of water inlet or outlet gates for FPC group. T-type thermocouples (with accuracy of 2%) were used to measure the inlet temperature and outlet temperature of each groups, as well as the ambient temperature. All measurement data is collected by a JTRG-II building thermal temperature automatic tester. And flow meters (with accuracy of 5%) were used to measure the flow of every FPC group. Testing started from 20:15 Mar. 11 to 7:00 Mar. 12, with 1 min recording interval.

3. Heat Loss Mathematical Model

In this paper, one group of FPCs in Fig.1 is the studying object for the heat loss mathematical model, which includes two pieces of FPCs and two pieces of connecting pipes.

3.1 Heat Loss Mathematical Model for the FPC

In nighttime, the total heat loss of FPC group equals the FPC heat loss plus the connecting pipes heat loss plus the FPC group heat storage change. The heat loss equation can be written as Eq. (1):

$$Q_u = Q_{lh} + Q_p + \triangle Q_s \quad \text{(eq. 1)}$$

Where Q_u is the total heat loss of FPC group, W; Q_{lh}, Q_p and ΔQ_s denote the FPC heat loss, the connecting pipes heat loss, and the FPC group heat storage change, W. The FPC group heat storage is negligible, so we make an assumption that $\Delta Q_s = 0$.

The FPC heat loss can be calculated by the FPC lighting area, the total heat loss coefficient, the sheet absorber temperature and environment temperature (Eq. (2)).

$$Q_{lh} = A_a U_L (T_a - T_e) \quad \text{(eq. 2)}$$

Where the A_a is the FPC lighting area, m^2. The U_L is the total heat loss coefficient, W/m^2·K. The T_a and T_e are the sheet absorber temperature and environment temperature，K。

The total heat loss coefficient is a comprehensive and equivalent value that integrate the front heat loss coefficient, the bottom heat loss coefficient, and the side heat loss coefficient (Eq. (3)).

$$U_L = U_t + U_b + \frac{A_e}{A_a} U_e \quad \text{(eq. 3)}$$

Where the U_t、U_b、U_e denote the front, bottom and side heat loss coefficient, W/m^2·K. The A_e denote the FPC side area, m^2.

The U_t is calculated by the formula (Eq. (4)-Eq. (7)) put forward by Klein (S.A. Klein, 1975), which has

considered the heat loss caused by cold radiation of the sky. And the error of the formula can be controlled in ± 0.3W/(m2 • K)。

$$U_t=\left[\frac{N}{\left(\frac{c}{T_p}\right)\left(\frac{T_a-T_e}{N+f}\right)^e}+\frac{1}{h_w}\right]^{-1}+\frac{\sigma\left(T_a^2+T_e^2\right)\left(T_a+T_e\right)}{\left(\varepsilon_p+0.00591Nh_w\right)^{-1}+\frac{2N+f-1+0.133\varepsilon_p}{\varepsilon_g}-N} \quad \text{(eq. 4)}$$

$$f=\left(1+0.089h_w-0.1166h_w\varepsilon_p\right)\left(1+0.07866N\right) \quad \text{(eq. 5)}$$

$$C=520\left(1-0.000051s^2\right) \quad \text{(eq. 6)}$$

$$e=0.43\left(1-100/T_a\right) \quad \text{(eq. 7)}$$

Where the N is the glass cover-plate number. The h_w is the convective heat transfer coefficient between the air and the surface. The ε_p and ε_g are the sheet and glass cover-plate absorber emissivity. The s is the installation angle of FPC.

The U_b and U_e can be calculated by Eq. (8) and Eq. (9).

$$U_b=1\Big/\left(\frac{1}{h_b}+\frac{1}{h_w+h_r}\right) \quad \text{(eq. 8)}$$

$$U_e=1\Big/\left(\frac{1}{h_e}+\frac{1}{h_w+h_r}\right) \quad \text{(eq. 9)}$$

Where the h_b, h_e and h_r are bottom, side, and radiation heat loss heat transfer coefficient, W/ m^2·K. We made the assumption that $h_r \approx 0$ (Y. Lu et al., 2013). The h_w can be achieved by outdoor wind speed (Li Ming, 2004), which is 1m/s according to Chengdu Tianqi net (Chengdu weather net, 2017).

$$h_w=5.7+3.8v \quad \text{(eq. 10)}$$

Because the sheet absorber is too big and has a non-uniform distribution of temperature, we introduce efficiency factor *F'* for modification (JA Duffie et al., 1980), in order to use the inlet and outlet average temperature instead of the sheet absorber temperature (Eq. (11)).

$$Q_{lh}^{'}=A_aU_LF'(T_f-T_e) \quad \text{(eq. 11)}$$

Where the T_f is the inlet and outlet average temperature (Eq. (12)).

$$T_f=\frac{T_{fi}+T_{fo}}{2} \quad \text{(eq. 12)}$$

Where the T_{fi} and the T_{fo} denote the inlet and outlet temperature.

FPC pipe and sheet absorber has three kinds of welding method, welding way adopted in the experiment are shown in figure 2. The *F'* for this kind of welding can be got through Eq. (13).

$$F'=1\Big/\left(\frac{WU_L}{h_i\pi D_i}+\frac{W}{D_o+(W-D_o)F}\right) \quad \text{(eq. 13)}$$

Where the W, D_i and D_o denote the sheet absorber width, the FPC pipe inner diameter and outer diameter, m.

The h_i is the convective heat transfer coefficient between the water and the FPC pipe wall, W/ m^2·K. The F is the sheet absorber efficiency. And the h_i has a connection with the inlet and outlet average temperature, the flow velocity, and the FPC pipe inner diameter (Eq. (14)) (Badescu V, 2006).

$$h_i = \left(1430 + 23.3T_f - 0.048T_f^2\right) v_w^{0.8} D_i^{-0.2} \quad \text{(eq. 14)}$$

Where the v_w is the flow velocity for FPC pipes, m/s. The F can be got through Eq. (15).

$$F = th\left[\frac{\sqrt{U_L/\lambda_a\delta}(W-D_o)}{2}\right] \Big/ \frac{\sqrt{U_L/\lambda_a\delta}(W-D_o)}{2} \quad \text{(eq. 15)}$$

Where the λ_a is the sheet absorber thermal conductivity, W/m·K . The δ is the Sheet absorber thickness.

3.2 Heat Loss Mathematical Model for the connecting pipes

The two connecting pipes are symmetrical in the PFC group, so it is assumed that the inlet and outlet average temperature is equal to the average temperature for connecting pipes. The connecting pipes heat loss can be calculated by Eq. (16)

$$Q_p = q_l l \quad \text{(eq. 16)}$$

Where the q_l is the heat loss of unit length, W/m. The l is the length of connecting pipes. The q_l can be got by the formula of thermal conductivity for a cylindrical wall (Eq. (17)).

$$q_l = (T_f - T_e) / \left(\frac{1}{h_i' D_i' \pi} + \frac{1}{2\pi\lambda} + \frac{1}{h_w D_o' \pi}\right) \quad \text{(eq. 17)}$$

Where the D_i' and D_o' denote the connecting pipe inner diameter and outer diameter, m. The v_w' denote the flow velocity for connecting pipes, m/s. The λ is the connecting pipe wall thermal conductivity, W/m·K. The h_i' is the convective heat transfer coefficient between the water and the connecting pipe wall, and can be obtained by Eq. (18).

$$h_i' = \left(1430 + 23.3T_f - 0.048T_f^2\right) v_w'^{0.8} D_i^{-0.2} \quad \text{(eq. 18)}$$

3.3 Heat Loss Mathematical Model for the working fluid

The heat loss for working fluid circulating within the FPC group can be calculated by the flow rate and the inlet and outlet temperatures (Eq. (19)), which are obtained directly by the experiment.

$$Q_u' = \rho c V (T_{fi} - T_{fo}) \quad \text{(eq. 19)}$$

Where the ρ and c are the density(kg/m^3) and specific heat capacity of water(J/(kg·K)). The V is the flow rate of the connect pipe.

3.4 Anti- freezing Analysis Method

According to the energy conservation law, the heat loss for heat carrying fluid flowing through the FPC group is equals to the total heat change of FPC group (20).

$$Q_u' = Q_u \quad \text{(eq. 20)}$$

From the Eq. (1)-Eq. (20), We can get the relationship among all the major parameters, which include the T_e, the T_{fi}, the T_{fo}, and the flow rate of FPCs. If we set outlet temperature equal to 0 as the critical condition of pipe freezing, we can obtain the critical flow rate in different environment temperature and inlet temperature.

4. Results and Discussion

4.1 Experimental Results

During the experiment, the flow rate for FPC group 1 and 2 were 3.09L/min and 1.67 L/min. The T_{fi} and T_{fo} for each group and the T_e are showed in Fig. 3. The Fig. 3 indicates that the inlet temperatures for the two group were similar, while the outlet temperature for FPC group 1 was higher than that for FPC group 2. It was because the flow rate for FPC group 1 was higher than that for FPC group 2, making heat transfer time shorter for every unit of fluid.

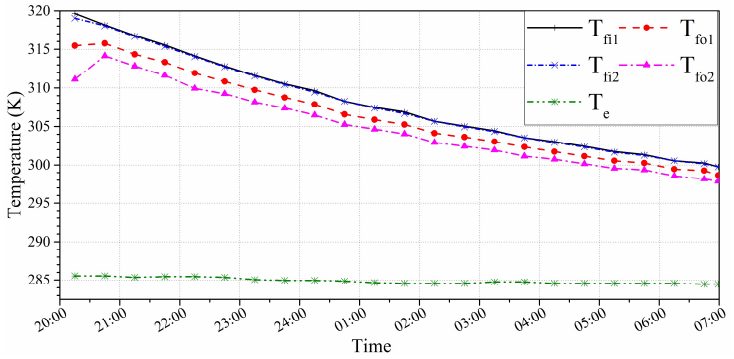

Fig. 3: Environment temperature, inlet temperature, and outlet temperature for every minute

In general, heat storage water tank has a limited capacity. With the operation of the anti-freezing working at nighttime, the inlet temperature become lower and lower, calling for a higher flow rate. So, it makes a difference to investigate the critical flow rate, which leads to the system antifreeze, in different environment temperature and inlet temperature.

Fig.4 shows the proportions of the PFC group front, bottom, side heat loss, and the connecting pipe heat loss. The front part of the PFC group occupied 62.32% of the heat loss, which constitutes the dominant part, because the cold radiation was large at night, and the top surface was large and has no heat insulation layer. The side part of the PFC group accounted for 3.57% of the heat loss, which serves as the smallest part, because the side surface was small and had a good heat insulation layer. The bottom part of the PFC group accounted for 18.57% of the heat loss, which was much smaller than the front part but had the same surface area as the front part. It was because of the bottom surface had a good heat insulating, substantiating the importance of heat insulating measures. The connecting pipes of the PFC group accounted for 15.53% of the heat loss, which was higher than the side part but lower than underside part. It was because of the connect pipe has no heat insulating layer, and was made by copper which had a high absorber thermal conductivity. In summary, reducing the heat loss in front part and making insulation layer for connecting pipes in practical engineering are very important, otherwise, the high heat loss of PFC groups will cause the outlet temperature too small, inevitably increasing the risk of system freezing.

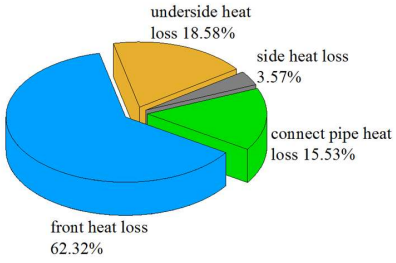

Fig. 4: The proportions of the PFC group front, bottom, side heat loss, and the connecting pipe heat loss

4.2 model verification

To verify the aforementioned heat loss mathematical model, we use Eq. (20) to compare the total heat loss of FPC (Q_u) with the heat loss for heat carrying fluid flowing through the FPC group (Q'_u).

Fig. 5 is the minutely variation of the Q_u and the Q'_u for the two groups. The Q_u and the Q'_u decrease gradually along the process of FPC groups dissipating heat at night. While the Q_{u1} is higher than Q_{u2} in most time, implying that the flow rate will be higher with the increase of the heat loss of the FPC group. Besides, since the Q_{u1} is always close and fit well to Q'_{u1}, so does the Q_{u2} to Q'_{u2}, the heat loss mathematical model can well describe the FPC group cooling process.

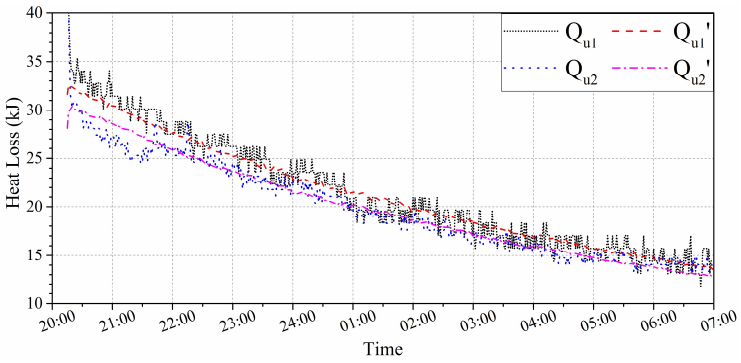

Fig. 5: The minutely variation of the Q_u and the Q'_u for the two groups

Fig. 6 is the cumulative variation of the Q_u and the Q'_u for the two groups. The $\sum Q_{u1}$ for one time is the cumulative Q_u before the time, so does the $\sum Q_{u2}, \sum Q'_{u1}, \sum Q'_{u2}$ to Q_{u2}, Q'_{u1}, Q'_{u2}. The $\sum Q_{u1}$ and the $\sum Q_{u2}$ increase gradually along the process of FPC groups dissipating heat at night. While the $\sum Q_{u1}$ is higher than $\sum Q_{u2}$ in most time, implying that the flow rate will be higher with the increase of the heat loss of the FPC group. Besides, the $\sum Q_{u1}$ is always close and fit well to $\sum Q'_{u1}$ with an error of only 1%, so does the $\sum Q_{u2}$ to $\sum Q'_{u2}$, so the heat loss mathematical model can well describe the FPC group cooling process, and the model can be used to study the heat loss of FPC group anti-freezing process.

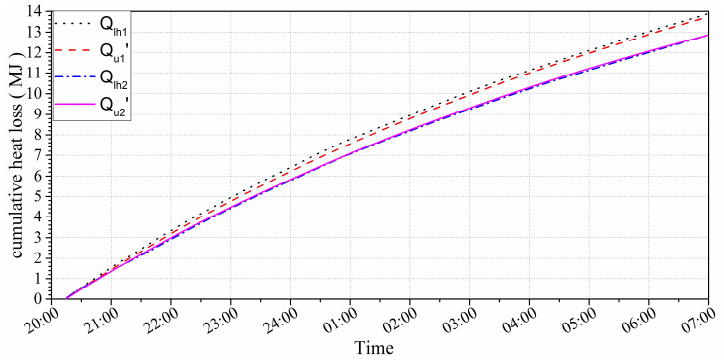

Fig. 6: The cumulative variation of the Q_u and the Q'_u for the two groups

4.3 Anti-freezing analysis for FPC group

In practical engineering, when the PFC group outlet temperature is lower than 0℃, the water in the system will be frozen. We define the flow rate of the system leading to 0℃ outlet temperature as the anti-freezing critical flow rate. When the inlet and ambient temperatures are constant, the heat loss increases with increasing flow rate, so the outlet temperature will be higher than 0℃ when the flow rate is higher than the anti-freezing critical flow rate.

Fig. 7 shows the anti-freezing critical flow rate varies with the ambient temperature and the inlet temperature. When the ambient temperature is constant, with the increase of inlet temperature, the anti-freezing critical flow rate is decreased fast when the inlet temperature is lower than 15℃ and is decreased slowly when the inlet temperature is higher than 15℃. When the inlet temperature is constant, with the increase of environment temperature, the anti-freezing critical flow rate is decreased fast when the inlet temperature is small and is decreased slowly when the inlet temperature is large. When the inlet temperature is 5℃, the anti-freezing critical

flow rate is decreased by 0.2L/min when the environment temperature is increased by 5℃. While when the inlet temperature is 30℃, the anti-freezing critical flow rate is decreased very slow when the environment temperature is increased.

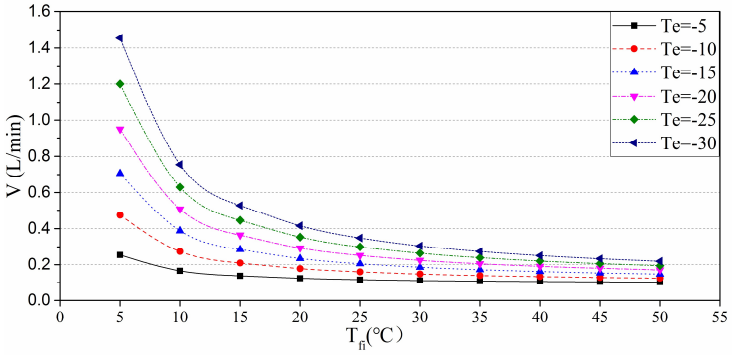

Fig. 7: The anti-freezing critical flow rate varies with the environment temperature and the inlet temperature

According to the standard (Hu Hanxin, 2016), the flow rate of the FPC group in daytime working is 4.8L/min, which is three times higher than the maximum anti-freezing critical flow rate in Fig. 7. In other words, the anti-freezing critical flow rate at night is much lower than the flow rate in daytime, so making anti-freezing flow rate equal to daytime working design flow rate is not a reasonable and desirable choice. By contrast, the flow rate should be reduced through the water pump frequency conversion methods.

4.4 Illustrative Example

We choose Harbin as a case of typical anti-freezing analyzing city, which is located in severe cold area of China and has the minimum temperature of -28.7℃ (U.S. Department of Energy and Lawrence Berkeley National Laboratory, 2017) in winter. Studying the anti-freezing critical flow rate in the winter extreme temperature of Harbin can provide meaningful references for practical engineering.

Fig.8 is the outlet temperature varies with the inlet temperature and flow rate in the winter extreme temperature. When the outlet temperature equals 0℃, the flow rate is the anti-freezing critical flow rate. Firstly, when the inlet temperature is constant, as the flow rate is increased, the outlet temperature is increased faster. Besides, when the flow rate is constant, as the inlet temperature is increased, the outlet temperature is increased. And when the flow rate is 1.5L/min, the outlet temperature is increased by 8℃ when the inlet temperature is increased by 5℃. Furthermore, when the inlet temperature ranges from 5℃ to 15℃, the anti-freezing critical flow rate is increased very fast when then inlet temperature is decreased, which is unfavorable for the anti-freezing flow rate control. So, in that situation, the inlet temperature should be higher than 15℃, and the anti-freezing flow rate should be higher than 0.5L/min.

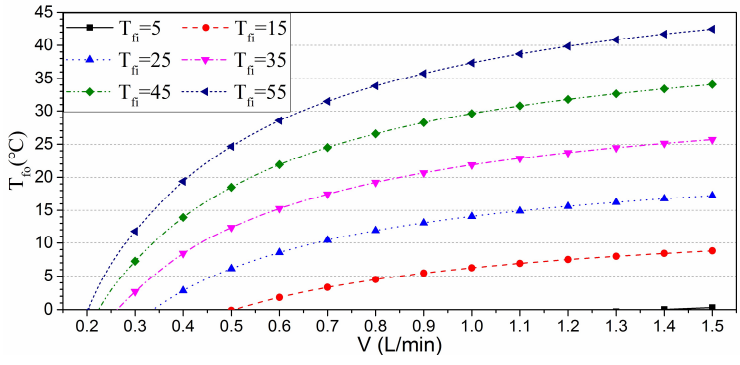

Fig. 8: The outlet temperature varies with the inlet temperature and flow rate in the winter extreme temperature

4. Conclusion

This paper studied the heat loss characteristic of the solar connector groups in nighttime through a heat loss mathematical model. A test bench which included two FPC groups has been built and solved analytically. The measured data well validated the analytical model. And main conclusions of this paper are as follows:

Firstly, when the FPC groups is anti-freezing working at night and the inlet temperature is constant, the outlet temperature increased when the flow rate increased, which keeps the system from freeze. But heat loss of FPC groups also increased when the flow rate increased. Secondly, the front part of the PFC group and connect pipes respectively accounted for 62.32% and 15.53% of the total heat loss, so reducing the heat loss in front part and making insulation layer for connecting pipes in practical engineering can make sense. But there is a pity that the front heat loss coefficient (Eq. (4)) did not independently show the radiant heat loss and the heat conduction, which is worth a further study. Besides, making anti-freezing flow rate equal to daytime working design flow rate is not suitable. By contrast, the flow rate should be reduced through the water pump frequency conversion methods. Furthermore, in the winter extreme temperature of Harbin, where the minimum temperature is -28.7℃, the input temperature should be higher than 15℃, and the anti-freezing flow rate should be higher than 0.5L/min.

This study can provide meaningful references for practical PFC groups anti-freezing engineering.

5. Acknowledgements

This project is funded by the National Key Research and Development Program (2016YFC00406), and the National Natural Science Foundation of China (No.51478280).

6. References

B.V. Bourke, 1995. Solar collector with freeze damage protection (P), in: United States Patent 5413091

Badescu V, 2006. Optimum fin geometry in flat plate solar collector systems (J). Energy Conversion and Management, v 47, n 15-16, p 2397-2413

BillyAnak Sup, TantiZanariahShamshir Ali, MohdFarid Zainudin, RosliAbu Bakar, 2014. Experimental study of water heating efficiency between aluminium and copper absorber plate in solar flat plate collector (J). Applied Mechanics and Materials, v 660, p 709-713

CJ Porras-Prieto, FR Mazarrón, VDL Mozos, JL García, 2014. Influence of required tank water temperature on the energy performance and water withdrawal potential of a solar water heating system equipped with a heat pipe evacuated tube collector (J). Solar Energy, v 110, p 365-377

Chengdu Tianqi Net, 2017. Chengdu Weather Net (EB/OL), in: http://chengdu.tianqi.com/20170311.html, 2017-3-12

F. Dinter, D. Mayorga Gonzalez, 2014. Operability, reliability and economic benefits of CSP with thermal energy storage: first year of operation of ANDASOL 3 (J). Energy Procedia, v 49, p 2472-2481

Fan Zhou, Jie Ji, Jingyong Cai, Bendong Yu, 2017. Experimental and numerical study of the freezing process of flat-plate solar collector (J). Applied Thermal Engineering, v 118, p 773-784

Gao Liuhua, Zhao Jun, Gao, Teng, 2014. Effect of absorber plate parameter on thermal performance of flat plat solar collector (J). Taiyangneng Xuebao/Acta Energiae Solaris Sinica, v 35, n 10, p 2054-2059

HMS Hussein, MA Mohamad, AS El-Asfouri, 1999. Optimization of a wickless heat pipe flat plate solar collector (J). Energy Conversion and Management, v 40, n 18, p 1949-1961

Huifang Liu, Shicong Zhang, Yiqiang Jiang, Yang Yao, 2014. Feasibility study on a novel freeze protection strategy for solar heating systems in severely cold areas (J). Solar Energy, v 112, p 144-153

Hu Hanxin, 2016. Design Standard for Heating and Ventilation of Civil Buildings in Sichuan Plateau-cold Zone (S). Northwestern Polytechnical University Press, Sichuan.

JA Duffie, WA Beckman, J Mcgowan, 1980. Solar Engineering of Thermal Processes (J). Journal of Solar Energy

Engineering, v 116, n 1, p 549

Li Ming, 2004. Theoretical and experimental analysis of the property of solar solid adsorption ice maker (J). Taiyangneng Xuebao/Acta Energiae Solaris Sinica, v 25, n 4, p 503-508

L.M. Ayompe, A. Duffy, S.J. McCormack, M. Conlon, 2011. Validated TRNSYS model for forced circulation solar water heating systems with flat plate and heat pipe evacuated tube collectors (J). Applied Thermal Engineering, v 31, n 8-9, p 1536-1542

M. Smyth, P. Eames, B. Norton, 2001. Evaluation of a freeze resistant integrated collector/storage solar water-heater for northern Europe (J). Applied energy, v 68, n 3, p 265-274

PW Cronin, PH Ottmar, EF Root, HM Simmons, 1997. Solar collector automatic freeze protection system (P), in: United States Patent 4044754

R.H. Lewis, Jr., J.B. Carr, 1981. Drain down freeze prevention control system for a solar collector (P), in: United States Patent 4256089

S.A. Klein, 1975. Calculation of flat-plate loss coefficients (J). Solar Energy, v 17, n 1, p 79

Th. Beikircher, P. Osgyan, S. Fischer, H. Druck, 2014. Short-term efficiency test procedure for solar thermal collectors based on heat loss measurements without insolation and a novel conversion towards daytime conditions (J). Solar Energy, v 107, p 653-659

U.S. Department of Energy and Lawrence Berkeley National Laboratory, 2017. EnergyPlus Energy Simulation Software (EB/OL), in: https://energyplus.net/weather-region/asia_wmo_region_2/CHN, 2017-10-10

Xiaolei Li, Ershu Xu, Shuang Song, Xiangyan Wang, Guofeng Yuan, 2017. Dynamic simulation of two-tank indirect thermal energy storage system with molten salt (J). Renewable Energy, v 113, p 1311-1319

Yu Lu, Hongwen Yu, Haicheng Ding, Yanli Zhang, Zongming Liu, 2013. Mathematical modeling and simulation of thermal properties of flat-plate solar collector (J). JOURNAL OF UNIVERSITY OF JINAN, v27, n3, p 293-297